Proc. Natl. Acad. Sci. USA
Vol. 96, pp. 49–54, January 1999
Biochemistry

Mechanisms by which IκB proteins control NF-κB activity

SIMOS SIMEONIDIS*, DEBORAH STAUBER*, GUOYING CHEN*, WAYNE A. HENDRICKSON*†, AND DIMITRIS THANOS*‡

*Department of Biochemistry and Molecular Biophysics and †Howard Hughes Medical Institute, Columbia University, 630 West 168th Street, New York, NY 10032

Contributed by Wayne A. Hendrickson, November 13, 1998

ABSTRACT **The biological activity of the transcription factor NF-κB is differentially controlled by three IκB proteins, IκBα, IκBβ, and IκBε. We have examined the molecular basis for the differential inhibitory strengths of IκB proteins by constructing hybrid IκBs and found that the first ankyrin repeat of IκBα is responsible for its strong inhibitory effect. Swapping a putative β-turn within the first ankyrin repeat between the strong IκBα and the weak IκBβ inhibitors switches their *in vivo* inhibitory activity on NF-κB. The qualitatively distinct contacts made by this β-turn in IκBα and IκBβ with NF-κB determine the efficiency by which IκBs sequester NF-κB to the cytoplasm, thus explaining their distinct effects on gene activity.**

The transcription factor NF-κB orchestrates the activation of numerous genes involved in the control of cell activities in the immune system and is also vital for craniofacial, liver, and limb development in higher eukaryotic organisms. NF-κB exists in virtually all cell types in the form of dimeric complexes consisting of different members of the Rel family of proteins. In mammals, there are five Rel proteins, p50, p52, p65, c-Rel, and RelB, all of which share an amino-terminal 300 amino acid conserved region known as Rel Homology Region. This region is responsible for DNA binding, dimerization, and nuclear localization. Unlike most transcriptional activators, NF-κB resides in the cytoplasm and must therefore translocate to the nucleus to function. Association with the inhibitory IκB proteins tightly regulates the activity of NF-κB. These interactions have two functional consequences. First, NF-κB/IκB complexes are sequestered in the cytoplasm, because IκBs mask the nuclear localization signal (NLS) of NF-κB, presumably by means of direct protein–protein interactions, and secondly, IκBs can inhibit NF-κB DNA binding. In response to a large variety of extracellular stimuli, the IκB proteins, while still bound to NF-κB, are phosphorylated, ubiquitinated, and finally degraded by the proteasome. The free NF-κB translocates to the nucleus, where it activates gene transcription (reviewed in refs. 1–5).

The IκB family consists of three members, IκBα, IκBβ, and IκBε (6–10). Importantly, the carboxyl-terminal regions of the precursors for p50 and p52, p105, and p100, respectively, can also function as IκBs. Each member of the family contains six copies of a 33 amino acid module known as ankyrin repeat, which functions as a protein–protein interaction domain. The region carboxyl-terminal to the ankyrin repeats contains a proline (P), glutamate (E), serine (S), and threonine (T) (PEST) sequence regulating basal level protein turnover and is also required for inhibition of DNA binding, whereas the amino-terminal region is the signal responsive domain (2, 5). Despite their extensive structural similarities, IκBα, IκBβ, and IκBε exhibit substantial differences *in vivo* (10–13). Depending on the cell type and on the stimulus, IκBs respond differentially to NF-κB-inducing signals. In general, IκBα is rapidly degraded, whereas IκBβ and IκBε are degraded with slower kinetics (1, 4, 5). In addition, IκBs inhibit NF-κB with different efficiencies. For instance, IκBα is a stronger inhibitor of NF-κB than is IκBβ or IκBε (10, 13).

IκB proteins are not only responsible for cytoplasmic sequestration of NF-κB in resting cells, but they also associate with NF-κB in the nucleus, where they inhibit NF-κB DNA binding and promote transport of NF-κB to the cytoplasm, thus terminating transcription and resetting the switch (13–15). IκBα is a stronger inhibitor of nuclear NF-κB activity than IκBβ, whereas IκBε enters the nucleus inefficiently (10, 13). Evidence for a nuclear function for the IκBs was also provided by the prolonged appearance of NF-κB in the nucleus of induced fibroblasts derived from mice in which the IκBα gene has been inactivated (16, 17). Thus, IκBβ and/or IκBε cannot substitute for IκBα function *in vivo* in this case. However, in mice in which the IκBα coding sequence was replaced by IκBβ, thus resulting in a dramatic increase of the IκBβ protein levels, a full restoration of the $I\kappa B\alpha^{-/-}$ abnormalities was observed (18). Considering all of the above experiments, we are confronted with the question of whether there is a specialized function for each IκB protein *in vivo*, namely cytoplasmic vs. nuclear, or whether their specific effects are solely caused by qualitatively distinct interactions with NF-κB.

In this paper, we have examined the molecular basis for the differential inhibitory strengths of IκB proteins. We have constructed hybrid IκBs, and found that the first ankyrin repeat of IκBα is responsible for its strong inhibitory effect. Remarkably, swapping a putative β-turn within the first ankyrin repeat between the strong IκBα and the weak IκBβ inhibitors switches their *in vivo* inhibitory activity on NF-κB. We showed that this putative β-turn functions by determining the strength by which IκBs can sequester NF-κB to the cytoplasm and is not involved in the nuclear function of IκBs, which is controlled by their carboxyl terminus. Therefore, by localizing the two distinct functions of IκBs to different regions of the molecule, we have demonstrated that the different IκBs contact NF-κB in a qualitatively distinct manner, causing distinct effects on gene activity. Our results, taken together with the three-dimensional structures of the IκB/NF-κB complexes, reveal the mechanisms by which IκB proteins control NF-κB activity *in vivo*.

MATERIALS AND METHODS

Plasmid Constructions and Cell Transfection. The IκB hybrids and the β-turn swaps were generated by standard PCR mutagenesis by using the appropriate set of primers. The PCR products were subcloned into the PRSET and PCDNA3 vectors (Invitrogen) for bacterial and mammalian cell expression. The integrity of all plasmids was verified by sequence

The publication costs of this article were defrayed in part by page charge payment. This article must therefore be hereby marked "*advertisement*" in accordance with 18 U.S.C. §1734 solely to indicate this fact.

Abbreviations: NLS, nuclear localization signal; GST, glutathione *S*-transferase; CAT, chloramphenicol acetyltransferase; PEST, (P), glutamate (E), serine (S), and threonine (T).

‡To whom reprint requests should be addressed. e-mail: dt73@columbia.edu.

analysis. All other plasmids used in this study have been previously described (10, 13).

HeLa, P19, or COS cells were transfected by the calcium phosphate method as previously described (10). Transfections were carried out with the amounts of plasmids indicated in the figure legends, and in every case vector DNA was added as necessary to achieve a constant amount of transfected DNA. The inhibition index was derived from NF-κB inhibitory curves by using increasing amounts of transfected IκB-expressing plasmids. The amount of a given IκB-expressing plasmid required for half-maximal inhibition of NF-κB and/or the slope of the curve defines the inhibition index.

Electrophoretic Mobility Shift Assays and Recombinant Protein Expression. Bacterial PACYC BL21(DE3) cells were transformed with plasmids expressing the desired His-tagged proteins, and expression was induced by addition of 1 mM isopropyl-D-thiogalactoside during mid-logarithmic growth phase and grown for 3 hr at 37°C. His-tagged proteins were purified and dialyzed as previously described (13). Electrophoretic mobility-shift assays with recombinant proteins or with whole-cell extracts were carried out as previously described (10).

Western Blotting. Cell extracts were separated by SDS/PAGE and were transferred onto nitrocellulose membrane (Millipore) in a buffer containing 25 mM Tris/192 mM glycine/20% methanol for 3 hr at 80 V and 4°C. The blots were blocked for 1 hr in TBST (20 mM Tris, pH7.6/137 mM NaCl/0.1% Tween-20) containing 5% dry milk. The blots were washed in TBST and incubated with primary antibodies for p65, IκBα, IκBβ, and IκBε (Santa Cruz Biotechnology) for 1 hr at room temperature with shaking. The blots were washed in TBST and were incubated with secondary antibody (Santa Cruz Biotechnology), and proteins were visualized by chemiluminescence (Amersham).

RESULTS

The First Ankyrin Repeat of IκBα Confers Strong Inhibitory Properties on IκBβ and IκBε. To investigate whether there are structural determinants in IκBα, IκBβ, and IκBε that are responsible for their differential inhibitory activities on NF-κB, we constructed chimeric IκB molecules bearing the amino-terminal domain and the first three ankyrin repeats of each IκB fused to the last three ankyrin repeats and the carboxyl-terminal domain of the other IκBs (Fig. 1*A,* lines 1–9). These chimeric inhibitors were then tested for their ability to associate with NF-κB by performing glutathione *S*-transferase (GST) pull-down experiments. Fig. 1*B* shows that *in vitro*-translated and S^{35}-labeled $I\kappa B\alpha_{123}\beta_{456}$, $I\kappa B\alpha_{123}\varepsilon_{456}$, and $I\kappa B\varepsilon_{123}\beta_{456}$ specifically interact with GST-p65 and not with GST alone (Fig. 1*B,* lanes 8, 10, 18, and 7, 9, 17, respectively). Surprisingly, the two chimeras bearing the carboxyl-terminal half of IκBα ($I\kappa B\beta_{123}\alpha_{456}$, $I\kappa B\varepsilon_{123}\alpha_{456}$) and the $I\kappa B\beta_{123}\varepsilon_{456}$ hybrid did not interact with p65 (Fig. *1B,* lanes 12, 16, and 14, respectively) or with p50 or c-Rel (data not shown). Thus, interaction of an IκB with NF-κB requires certain combinations of ankyrin repeats, despite the extensive sequence similarity between the ankyrin repeats in the same position of each IκB (5). These results suggest that the three different IκBs interact with NF-κB by means of multiple interdependent contacts involving all ankyrin repeats. The latter is also supported by the observations that deletion of either the first or the last ankyrin repeats of either IκBα or IκBε eliminates their ability to interact with NF-κB (ref. 2; unpublished observations).

The ability of these chimeras to inhibit NF-κB *in vivo* was tested in cotransfection experiments by using the $PRDII_4$-chloramphenicol acetyltransferase (CAT) reporter (four copies of the NF-κB site taken from the IFN-β promoter) that was activated by a small constant amount of transfected NF-κB p65

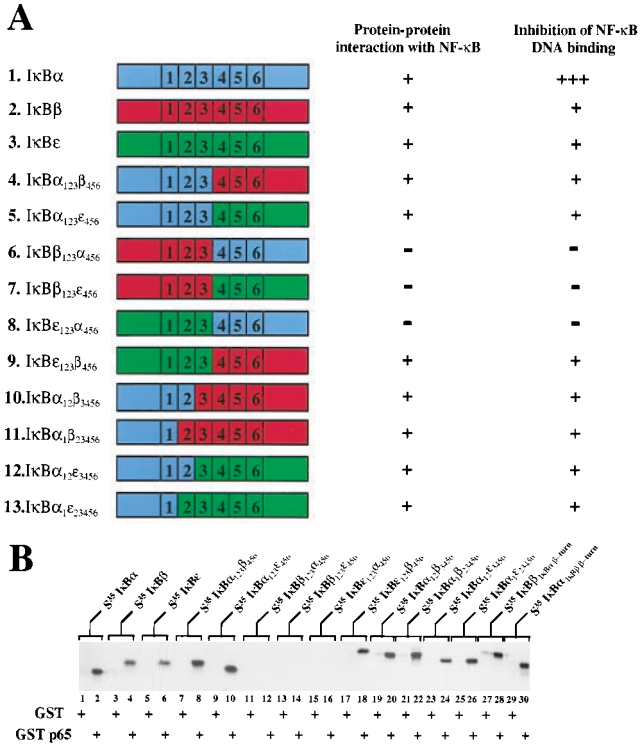

FIG. 1. Diagrammatic illustration of the IκB hybrids. (*A*) Diagrammatic illustration of the IκB hybrids used in this study. Shown on the right is a summary of their abilities to interact with NF-κB and to inhibit NF-κB DNA binding *in vitro*. (*B*) Protein–protein interactions between the indicated IκB hybrids and GST or GST-p65. The IκB hybrids indicated on the top of the autoradiogram were *in vitro* translated and ^{35}S labeled, and equal amounts were incubated with either glutathione beads harboring GST alone (odd lane numbers) or glutathione beads harboring GST-p65 (even lane numbers). The bound proteins were analyzed by PAGE and were visualized by autoradiography.

subunit along with increasing amounts of the IκB expression vectors. Fig. 2*B* shows that all different IκB proteins are accumulated at comparable amounts after transfection and Western blot analysis. Dose-dependent IκB inhibitory curves were obtained for all IκB expression vectors and the relative inhibitory strength of each IκB is depicted in Fig. 2*A* as inhibition index (see *Materials and Methods*). The inhibition index was arbitrarily set as 100 for IκBα, to which all other IκBs are compared. Fig. 2*A* shows that IκBα is a ≈7 and ≈14 times stronger inhibitor of NF-κB than IκBβ and IκBε (Fig. 2*A*, compare line 2 with 3 and 4, respectively), a result consistent with our previous experiments (10, 13). Remarkably, $I\kappa B\alpha_{123}\varepsilon_{456}$ is a three times stronger inhibitor than IκBα (Fig. 2*A*, line 5), whereas $I\kappa B\alpha_{123}\beta_{456}$ is as strong as IκBα (Fig. 2*A*, line 6). As expected, the three chimeras that fail to interact with p65 did not inhibit p65-dependent transcriptional activation (Fig. 2*A*, lines 7–9). Finally, the $I\kappa B\varepsilon_{123}\beta_{456}$ hybrid inhibits p65 as efficiently as does IκBε (Fig. 2*A*, line 10). Identical results were obtained either by using the p50/p65 heterodimer as an activator or the endogenous NF-κB proteins that were induced after TNF-α treatment (data not shown). These experiments strongly suggest that the strength by which different IκBs inhibit NF-κB *in vivo* is determined primarily by their first three ankyrin repeats and/or the amino terminus.

IκB hybrids bearing either the first or the first plus the second ankyrin repeats of IκBα fused to the remaining ankyrin repeats of IκBβ and IκBε (Fig. 1*A*, lines 10–13) specifically interact with p65 (Fig. 1*B*, lanes 20, 22, 24, and 26), and they are also expressed at similar levels with the other IκBs after transfection (Fig. 2*B*, lanes 4, 5, 9, and 10). Interestingly,

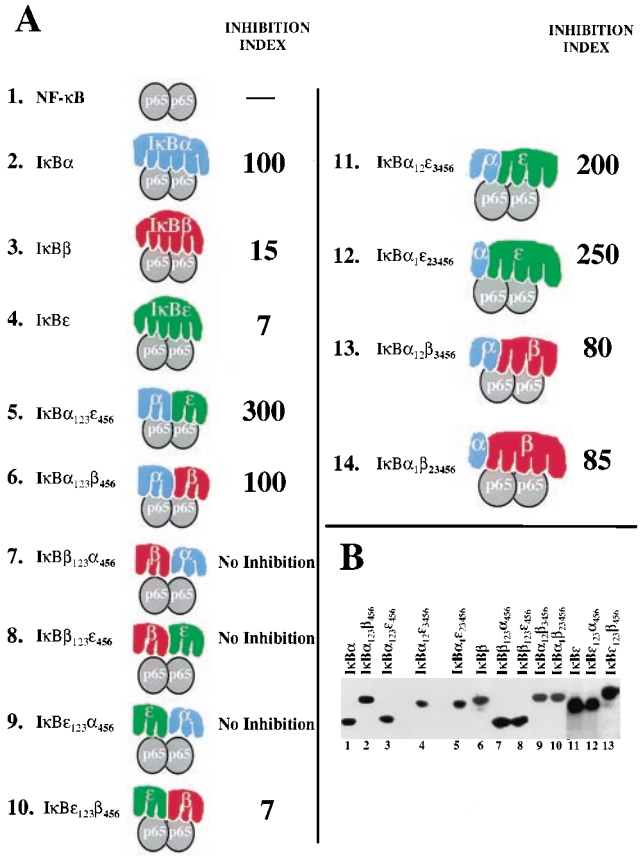

FIG. 2. The first ankyrin repeat of IκBα is sufficient to convert IκBβ and IκBε from weak to strong inhibitors of NF-κB activity *in vivo*. (*A*) P19 cells were transfected with the $PRDII_4CAT$ reporter plasmid (100 ng) along with a constant amount of CMV p65 expression vector (100 ng) and increasing amounts of the indicated IκB hybrids (10 ng, 30 ng, 100 ng, 300 ng, 1000 ng, and 3000 ng). The resulting CAT activities were plotted as a fraction of the IκB expression vector amount used in the transfection. The inhibition index was derived as described in *Materials and Methods* by averaging the results obtained from six independent experiments. The variability from experiment to experiment was less than 20%, whereas the variability between individual constructs in the same experiment was less than 5%. (*B*) Shown is a Western blot using whole cell extracts derived from cells transfected with the indicated IκB expression vectors that were immunoblotted with IκBα (lanes 1–5, 9–10), IκBβ (lanes 6–8), or IκBε (lanes 11–13), specific antibodies. All IκB hybrids display the expected size, indicating thus their integrity.

replacement of the first ankyrin repeat of IκBε or IκBβ by the first ankyrin repeat of IκBα is sufficient to convert IκBε and IκBβ from weak to strong inhibitors of NF-κB (Fig. 2*A*, lines 12 and 14). Thus, we have determined that the first ankyrin repeat of IκBα is sufficient for the strong inhibitory activity of IκBα on NF-κB.

Swapping a Putative β-Turn Between IκBα and IκBβ Switches Their Inhibitory Properties. Previous studies of the three-dimensional structure of ankyrin repeat-containing proteins established that the ankyrin repeat module adopts a conformation consisting of two antiparallel α-helices and a β-turn (19–22). Adjacent ankyrin repeats form a four-helix bundle with their β-turns positioned perpendicularly to the helices. The majority of the protein–protein interactions between the ankyrin repeat-containing proteins and their targets are mediated by the β-turn. Based on these observations, we modeled the first ankyrin repeat of IκBα and IκBβ and found that the putative β-turn in their first ankyrin repeat consists of four amino acids, two of which are different between these two proteins (Fig. 3 *A* and *B*). Importantly, the site of fusion between different IκBs in our hybrids lies immediately at the end of the putative β-turn. Therefore, we hypothesized that the difference in the inhibitory activity between IκBα and IκBβ could be caused by the distinct contacts made by this β-turn with NF-κB. To test this hypothesis, we constructed IκBα and IκBβ molecules in which this β-turn was swapped between the two inhibitors (Fig. 3*B*). The resulting IκBs ($I\kappa B\alpha_{I\kappa B\beta\ \beta\text{-turn}}$ and $I\kappa B\beta_{I\kappa B\alpha\ \beta\text{-turn}}$) were tested for their ability to inhibit NF-κB-dependent transcriptional activation in transfection experiments. Remarkably, the IκBβ molecule bearing the IκBα β-turn ($I\kappa B\beta_{I\kappa B\alpha\ \beta\text{-turn}}$) inhibited NF-κB almost as efficiently as IκBα (Fig. 3*C*, compare lines 1 and 4). That is, its inhibitory activity was enhanced 8-fold as compared with IκBβ (compare lines 3 and 4). By contrast, the IκBα molecule bearing the IκBβ β-turn ($I\kappa B\alpha_{I\kappa B\beta\ \beta\text{-turn}}$) inhibited NF-κB seven times more weakly than IκBα (Fig. 3*C*, compare lines 1 and 2). That is, its activity approximates the inhibitory properties of IκBβ (compare lines 2 and 3). The Western blot in Fig. 3*D* shows that these proteins are expressed at comparable levels in the cells. Thus, we established that the differential inhibitory properties of IκBα and IκBβ *in vivo* can be attributed to the distinct functional role of their β-turn, perhaps involving specific contacts with NF-κB. Our β-turn swap experiments also suggest that differences in basal phosphorylation of IκBα and IκBβ are not critical in determining their overall inhibitory strength.

The Strength by Which IκBs Inhibit NF-κB Correlates with Cytoplasmic Sequestration Rather than with Inhibition of NF-κB DNA Binding. The association between NF-κB and IκB proteins results in their mutual cytoplasmic sequestration and in inhibition of NF-κB DNA binding. The fact that IκBα is a stronger inhibitor of NF-κB DNA binding compared with IκBβ suggests that the putative β-turn we identified as a critical IκB inhibitory structural determinant may be directly involved in inhibition of NF-κB DNA binding. To test this idea, we carried out electrophoretic mobility-shift assay experiments using recombinant NF-κB p65 subunit and several IκB proteins that were expressed and purified to near homogeneity from bacteria (Fig. 4*B*). A constant amount of p65 was allowed to interact with the PRDII oligonucleotide and then was challenged with increasing amounts of IκB proteins. Consistently with our previous experiments, IκBα inhibited NF-κB DNA binding more efficiently than IκBβ and IκBε (Fig. 4*A*, compare lanes 2–5 with 6–9 and 10–13, respectively). Surprisingly, all the IκB chimeras bearing the first ankyrin repeat of IκBα, which are strong inhibitors of NF-κB activity *in vivo*, inhibited NF-κB DNA binding only weakly, resembling thus IκBβ or IκBε (Fig. 4*A,* lanes 14–17, 34–37, 38–41, and 42–45). In addition, $I\kappa B\beta_{I\kappa B\alpha\ \beta\text{-turn}}$, which is a strong inhibitor of NF-κB activity *in vivo*, inhibits NF-κB DNA binding only weakly (Fig. 4*A*, lanes 50–53). By contrast, $I\kappa B\alpha_{I\kappa B\beta\ \beta\text{-turn}}$, which is a weak inhibitor of NF-κB *in vivo*, is a strong inhibitor of NF-κB DNA binding *in vitro* (Fig. 4*A*, lanes 46–49). Thus, the efficiency by which a given IκB hybrid inhibits NF-κB DNA binding *in vitro* correlates with the identity and origin of the last three ankyrin repeats in the hybrid. For example, $I\kappa B\alpha_{123}\beta_{456}$ inhibits NF-κB as efficiently as IκBβ does (Fig. 4*A*, compare lanes 14–17 and 6–9). As expected, the hybrids that did not interact with p65 also did not affect its DNA binding activity (Fig. 4*A*, lanes 18–21, 22–25, and 26–29). Therefore, the carboxyl half of a given IκB determines the strength by which it can inhibit NF-κB DNA binding *in vitro*. Taken together, these experiments suggest that there is no correlation between the strength by which IκBs inhibit the NF-κB activity *in vivo* and NF-κB DNA binding *in vitro*. Furthermore, using p65 derivatives that can bypass cytoplasmic sequestration by co-expressed IκBs (10, 13), we demonstrated that the efficiencies by which the hybrid IκBs inhibit NF-κB DNA binding *in vivo* correlate with the efficiency by which they inhibit NF-κB DNA binding *in vitro* (data not shown). Finally, these experiments

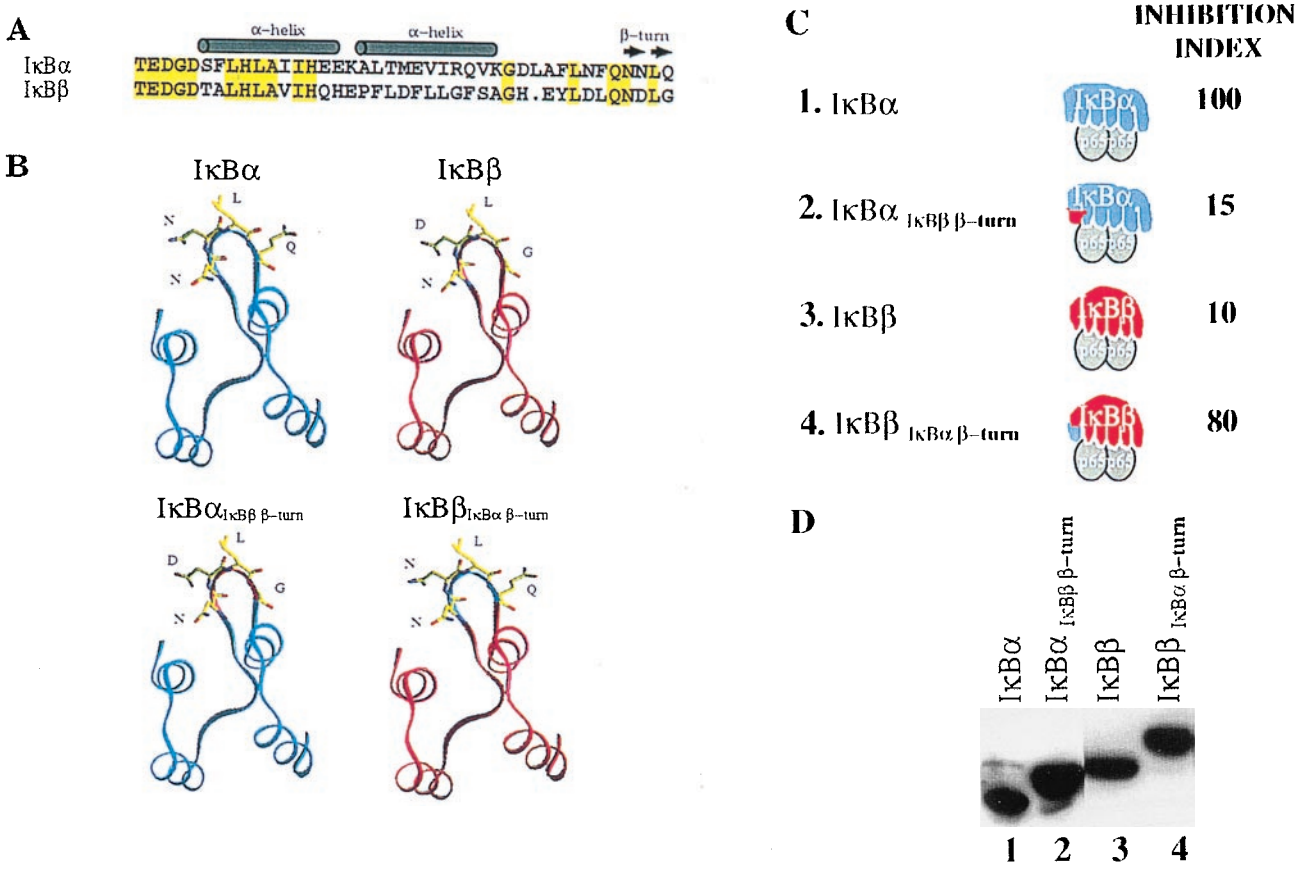

FIG. 3. Swapping a putative β-turn between IκBα and IκBβ switches their inhibitory activities. (*A*) Sequence alignment and secondary structure prediction of the first ankyrin repeat of IκBα and IκBβ. Identical amino acids are indicated in yellow. (*B*) Model building of the first ankyrin repeat of IκBα and IκBβ performed by using O (28). Coordinates for GABPβ (21) and 53BP2 (19) were obtained from the Protein Data Bank (29). When modeling IκBα and IκBβ, the same backbone dihedrals were used and side chain rotamers were built such that the rotamer matched that of the crystal structures. (*C*) P19 cells were transfected as outlined in Fig. 2 along with expression vectors encoding the $I\kappa B\alpha_{I\kappa B\beta\ \beta\text{-turn}}$ and $I\kappa B\beta_{I\kappa B\alpha\ \beta\text{-turn}}$ inhibitors. The inhibition index was derived from five independent experiments and the variability was less than 20%. (*D*) Shown is a Western blot verifying the comparable expression of the indicated IκB proteins after transfection. The slightly larger size (2 kDa) of the swapped constructs compared with their wild-type counterparts is caused by the presence of the six histidine tag moiety at their amino termini.

also revealed that inhibition of the NF-κB DNA-binding activity in the nucleus by IκBs represents only a very small fraction (≈10%) of their overall inhibitory potential and cannot therefore explain their differential inhibitory strengths (data not shown) because only a small fraction of IκB proteins can enter the nucleus (10, 11, 13, 14).

Next, we examined whether the difference in the inhibitory strength of IκBs on NF-κB can be explained by the efficiency by which they sequester NF-κB in the cytoplasm. A constant amount of p65 expression vector was transfected into the cells, along with a constant amount of expression vectors encoding IκB proteins with different inhibitory strengths. These amounts were chosen after preliminary titration experiments to ensure that IκBs are not accumulated in excess of p65 (data not shown). Nuclear and cytoplasmic extracts were prepared, and the amount of p65 present in each compartment was determined by Western blot analysis. In parallel, we determined the ability of each IκB to inhibit NF-κB transcriptional activity. Fig. 5 shows that transfection of p65 leads to its nuclear accumulation and activation of transcription (Fig. 5, lane 2). Cotransfection of p65 and IκBα expression vectors results in reduction of nuclear p65, which is accompanied by a strong decrease in transcriptional activation (Fig. 5, lane 3). However, cotransfection of p65 along with either IκBβ, IκBε, or $I\kappa B\alpha_{I\kappa B\beta\ \beta\text{-turn}}$ did not significantly reduce nuclear accumulation of p65, nor did it decrease p65-dependent transcriptional activation (Fig. 5, compare lane 2 with lanes 4, 5, and 8). By contrast, $I\kappa B\alpha_{123}\beta_{456}$, $I\kappa B\alpha_{123}\varepsilon_{456}$, and $I\kappa B\beta_{I\kappa B\alpha\ \beta\text{-turn}}$ strongly restricted p65 to the cytoplasm, thus decreasing its transcriptional activation capacity (lanes 6, 7, and 9, respectively). Therefore, the ability of a given IκB protein to inhibit NF-κB *in vivo* directly correlates with its ability to sequester NF-κB to the cytoplasm and not with its relative ability to inhibit NF-κB DNA binding in the nucleus. Finally, the efficiency by which a given IκB sequesters NF-κB in the cytoplasm is primarily determined by interactions involving a putative β-turn at the end of their first ankyrin repeat.

DISCUSSION

A large number of previous studies have established that there is a division of labor among different NF-κB and IκB proteins. Thus, not only are distinct combinations of NF-κB proteins directed to specific promoters, but the different IκBs also display a gradient of inhibitory activities on different combinations of Rel complexes. We showed that the differential inhibitory activities of IκBα, IκBβ, and IκBε on NF-κB *in vivo* can be attributed, at least in part, to a putative β-turn located at the border between the first and second ankyrin repeats. Transfer of this putative β-turn from IκBα to IκBβ suffices to convert IκBβ from a weak to a strong inhibitor of NF-κB *in vivo* and vice versa. Unexpectedly, our experiments also revealed that the differential inhibitory activity of IκBs correlates with the efficiency by which they sequester NF-κB in the cytoplasm and not with the relative ability by which they inhibit NF-κB DNA binding in the nucleus. The molecular explana-

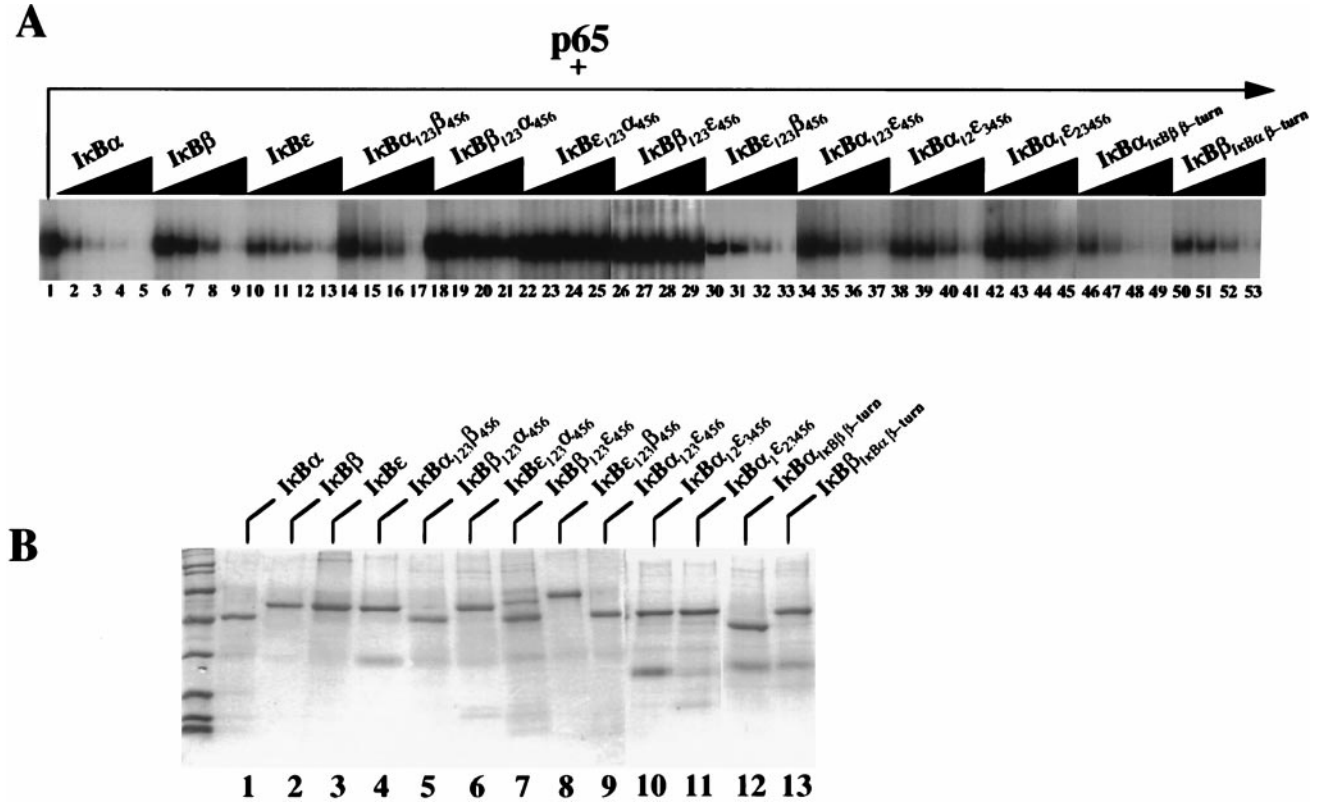

FIG. 4. Comparison of the effects of the IκB hybrids on NF-κB DNA binding. (*A*) Shown is an electrophoretic mobility-shift assay experiment performed with a constant amount of recombinant p65 in the presence or absence (lane 1) of the indicated recombinant IκB proteins. The molar ratio between p65 and IκB proteins was 1:2, 1:6, 1:18, and 1:54. (*B*) Shown is a Coomassie blue-stained SDS/PAGE gel displaying the purified IκB proteins used in this study.

tion for this latter observation is consistent with the fact that only a small fraction of IκB proteins can enter the nucleus, thus inhibiting NF-κB DNA binding to promoters (10, 13, 14, and data not shown). For example, the overall inhibition by $IκBα_{IκBβ\ β\text{-turn}}$ approximates that of IκBβ, despite the fact that $IκBα_{IκBβ\ β\text{-turn}}$ is a strong inhibitor of NF-κB DNA binding either *in vivo* or *in vitro*. We showed that this differential inhibitory activity is because of the lower efficiency by which these proteins sequester NF-κB in the cytoplasm. Therefore, we propose that the swapped putative β-turn is directly involved in the efficient sequestration of NF-κB in the cytoplasm, presumably by contacting the NLS and/or neighboring residues. Additional evidence for a qualitatively distinct interaction of IκBα and IκBβ with the NF-κB NLS region has been provided in previous studies by showing that the NF-κB NLS is more accessible to antibodies when NF-κB is complexed with IκBβ than with IκBα (11).

The recent determination of the IκB/NF-κB three-dimensional structures revealed that the putative β-turn we identified as a critical structural determinant of the IκBα/NF-κB interactions is indeed a β-turn, the second β-turn in IκBα structure, which makes contacts with the region lying immediately amino-terminal to the NLS of p65 and p50 (23, 24). Specific amino acids in this β-turn, $N_{108}N_{109}L_{110}Q_{111}$, are engaged in interactions with the NLS region of the p50 and p65 subunits, with N_{109} and Q_{111} contacting p50, whereas L_{110} contacts p65 (23). Our model of the β-turn (Fig. 3*B*) shows that the side chains at positions 1 and 3 project oppositely from those at positions 2 and 4 (N_{109} and Q_{111}), where changes were made. We showed that conversion of NNLQ (IκBα β-turn) to NDLG (IκBβ β-turn) weakens the ability of the resulting IκB to sequester NF-κB in the cytoplasm. As depicted in the crystal structure, N_{109} interacts with an isoleucine (I354) in p50 located just before the NLS (23). It is expected that conversion of this asparagine to aspartate, as in IκBβ, will affect this interaction. Similarly, conversion of Q_{111} to glycine will result in the loss of side-chain-mediated hydrogen bonds with the main chain of the same residue (I354). The other two amino acids in the β-turn (N_{108} and L_{110}), which are identical between IκBα and IκBβ, are primarily involved in the packing of the IκBα structure and most likely in IκBβ, with the exception of L_{110}, which makes a distant contact with K_{301} of p65 NLS. The first β-turn in the IκBα structure, which precedes the two helices, makes the contacts with the basic sequence $K_{301}R_{302}K_{303}R_{304}$, which is the NLS of p65 (23). Interestingly, this β-turn (EDGD) is absolutely conserved between IκBα, IκBβ, and IκBε, ensuring thus that all IκBs will contact NF-κB's NLS in a qualitatively similar manner. On the other hand, the sequence variability between different IκBs in the second β-turn is expected to cause qualitatively different types of contacts with the region immediately next to NLS. We demonstrated that the quality of these interactions is critical for determining the transcriptional activating potential of NF-κB *in vivo*, by showing that they control the efficiency by which IκBs sequester NF-κB in the cytoplasm. Thus, we propose that the interaction of the second β-turn of IκBs with the NLS region of NF-κB assists in the masking of the NF-κB NLS by IκB proteins. Other topologically distinct regions in IκB proteins, such as the amino terminus, may ordinarily be involved in interactions leading to cytoplasmic sequestration of NF-κB (25, 26). However, our β-turn swapping experiments revealed that these putative interactions are not critical in discriminating the strength by which IκBs sequester NF-κB in the cytoplasm.

Our experiments also provided new insights into the mechanism by which IκB proteins inhibit NF-κB DNA binding. We showed that IκB hybrids bearing the carboxyl half of IκBβ or IκBε fused to the amino half of IκBα inhibited NF-κB DNA

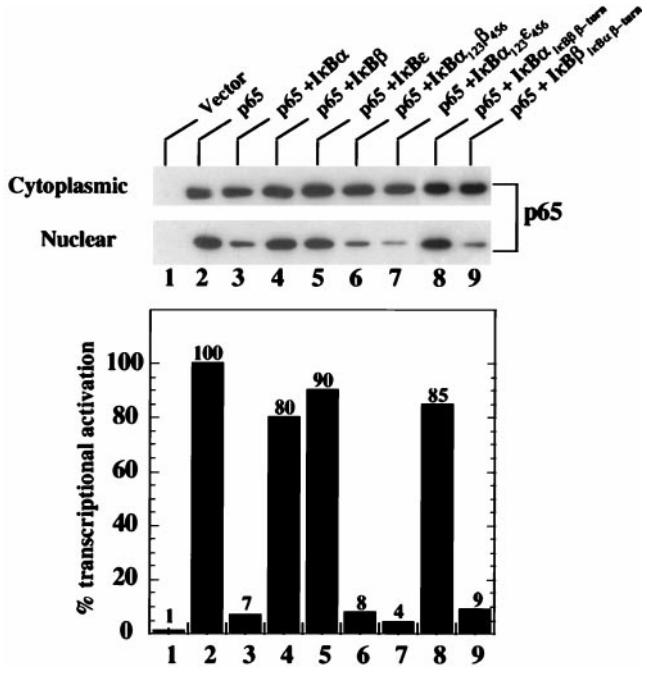

FIG. 5. Comparison of the effects of different IκB proteins in cytoplasmic sequestration of NF-κB. P19 cells were transfected with a constant amounts of p65 (3 μg) along with the indicated IκB expression vectors (17 μg). Nuclear and cytoplasmic extracts were prepared and immunoblotted with a p65 antibody. The bottom of the figure indicates the transcriptional activity obtained from the cotransfected $PRDII_4CAT$ reporter plasmid.

binding either *in vivo* or *in vitro* only weakly and with the same efficiency as IκBβ or IκBε, respectively. Thus, the strength by which IκBs inhibit NF-κB DNA binding is determined by their last three ankyrin repeats and their carboxyl terminus containing the acidic PEST sequence. Our observation is in absolute agreement with the topology of the latter region of IκBα relative to the NF-κB DNA-binding domain, as revealed by the crystal structure of the IκB/NF-κB complex (23, 24). As depicted in both structures, the last ankyrin repeat and the acidic carboxyl tail of IκBα are involved in contacts with the DNA binding domain of NF-κB. The importance of these contacts in IκB function was underscored in previous experiments showing that the carboxyl tail region of IκBα and IκBβ is critical in determining the strength by which they inhibit NF-κB DNA binding (13, 25–27). Thus, our experiments taken together with the structure of the IκBα/NF-κB complex reveal the mechanisms by which IκB proteins control NF-κB activity *in vivo*.

We are extremely grateful to Marc D. Jabobs, Stephen C. Harrison, and Gourisankar Ghosh for making available to us their IκB/NF-κB crystal structures before publication. We also thank Tom Maniatis and Richard Mann for critical reading of the manuscript and Junming Yie for help with the figures. This work was supported by an American Heart Association grant-in-aid, the Council for Tobacco Research-USA, Inc., the Pew Scholars Program in Biomedical Sciences, the Irma T. Hirschl Foundation, and partly by National Institutes of Health (1RO1GM54605) grants to D.T. W.A.H. is an investigator of the Howard Hughes Medical Institute.

1. Thanos, D. & Maniatis, T. (1995) *Cell* **80,** 529–532.
2. Verma, I. M., Stevenson, J. K., Schwarz, E. M., Van Antwerp, D. & Miyamoto, S. (1995) *Genes Dev.* **9,** 2723–2735.
3. Baeuerle, P. A. & Baltimore, D. (1996) *Cell* **87,** 13–20.
4. Baldwin, A. S., Jr. (1996) *Annu. Rev. Immunol.* **14,** 649–681.
5. Ghosh, S., May, M. J. & Kopp, E. B. (1998) *Annu. Rev. Immunol.* **16,** 225–260.
6. Haskill, S., Beg, A. A., Tompkins, S. M., Morris, J. S., Yurochko, A. D., Sampson-Johanne, A., Mondal, K., Ralph, P. & Baldwin, A. S. (1991) *Cell* **65,** 1281–1289.
7. Thompson, J. E., Phillips, R. J., Erdument-Bromage, H., Tempst, P. & Ghosh, S. (1995) *Cell* **80,** 573–582.
8. Whiteside, S. T., Epinat, J. C., Rice, N. R. & Israel, A. (1997) *EMBO J.* **16,** 1413–1426.
9. Li, Z. & Nabel, G. J. (1997) *Mol. Cell. Biol.* **17,** 6184–6190.
10. Simeonidis, S., Liang, S., Chen, G. & Thanos, D. (1997) *Proc. Natl. Acad. Sci. USA* **94,** 14372–14377.
11. Suyang, H., Phillips, R., Douglas, I. & Ghosh, S. (1996) *Mol. Cell. Biol.* **16,** 5444–5449.
12. Chu, Z.-L., McKinsey, T. A., Liu, L., Qi, X. & Ballard, D. W. (1996) *Mol. Cell. Biol.* **16,** 5974–5984.
13. Tran, K., Merika, M. & Thanos, D. (1997) *Mol. Cell. Biol.* **17,** 5386–5399.
14. Arenzana-Seisdedos, F., Thompson, J., Rodriguez, M. S., Bacherlerie, F., Thomas, D. & Hay, R. T. (1995) *Mol. Cell. Biol.* **15,** 2689–2696.
15. Arenzana-Seisdedos, F., Turpin, P., Rodriguez, M., Thomas, D., Hay, R. T., Virelizier, J.-L. & Dargemont, C. (1997) *J. Cell Sci.* **110,** 369–378.
16. Beg, A. A., Sha, W. C., Bronson, R. T. & Baltimore, D. (1995) *Genes Dev.* **9,** 2736–2746.
17. Klement, J. F., Rice, N. R., Car, B. D., Abbondanzo, S. J., Powers, G. D., Bhatt, H., Chen, C.-H., Rosen, C. A. & Stewart, C. L. (1996) *Mol. Cell. Biol.* **16,** 2341–2349.
18. Cheng, J. D., Ryseck, R.-P., Attar, R. M., Dambach, D. & Bravo, R. (1998) *J. Exp. Med.* **188,** 1055–1062.
19. Gorina, S. & Pavletich, N. P. (1996) *Science* **274,** 1001–1005.
20. Luh, F. Y., Archer, S. J., Domaille, P. J., Smith, B. O., Brotheron, D. H., Raine, A. R., Xu, X., Brizuela, L., Brenner, S. L. & Laue, E. D. (1997) *Nature (London)* **389,** 999–1003.
21. Batchelor, A. H., Piper, D. E., de la Brousse, F. C., McKnight, S. L. & Wolberger, C. (1998) *Science* **279,** 1037–1041.
22. Venkataramani, R., Swaminathan, K. & Marmostein, R. (1998) *Nat. Struct. Biol.* **5,** 74–81.
23. Jacobs, M. D. & Harrison, S. C. (1998) *Cell,* in press.
24. Huxford, T., Huang, D.-B., Malek, S. & Ghosh, G. (1998) *Cell,* in press.
25. Latimer, M., Ernst, M. K., Dunn, L. L., Drutkaya, M. & Rice, N. R. (1998) *Mol. Cell. Biol.* **18,** 2640–2649.
26. Luque, I. & Gelinas, C. (1998) *Mol. Cell. Biol.* **18,** 1213–1224.
27. Ernst, M. K., Dunn, L. L. & Rice, N. (1995) *Mol. Cell. Biol.* **15,** 872–882.
28. Jones, T. A., Zou, J.-Y., Cowan, S. W. & Kjeldgaard, M. (1991) *Acta Crystallogr. A* **47,** 110–119.
29. Bernstein, F. C., Koetzle, T. F., Williams, G. J. B., Meyer, E. J., Jr., Brice, M. D., Rodgers, J. K., Kennard, O., Shimanouchi, I. & Tasumi, M. (1978) *Arch. Biochem. Biophys.* **185,** 584–591.